Nat. Hazards Earth Syst. Sci. Discuss., 2, 3251–3288, 2014
www.nat-hazards-earth-syst-sci-discuss.net/2/3251/2014/
doi:10.5194/nhessd-2-3251-2014

Natural Hazards and Earth System Sciences
Open Access
Discussions

A validation of an operational wave and surge prediction system for the Dutch Coast

L. Sembiring[1,2], **M. van Ormondt**[2], **A. van Dongeren**[2], **and D. Roelvink**[1,2]

[1]UNESCO-IHE Institute for Water Education, Delft, the Netherlands
[2]Deltares, Delft, the Netherlands

Received: 12 March 2014 – Accepted: 22 April 2014 – Published: 9 May 2014

Correspondence to: L. Sembiring (l.sembiring@unesco-ihe.org)

Published by Copernicus Publications on behalf of the European Geosciences Union.

Abstract

Knowledge of the actual condition of hydrodynamics in the nearshore and coastal area is essential for coastal monitoring activities. To this end, a coastal operational model system can serve as a tool in providing recent and up-to-date state of the hydrodynamics along the coast. In this paper we apply CoSMoS (Coastal Storm Modeling System), a generic operational model system applied here to predict storm impact on dunes along the Dutch Coast. The CoSMoS application is not limited to storm impact prediction on the Dutch coast, but can also be applied to other coastal hazards such as rip currents and coastal flooding, in other environments. In this paper, we present the setup of the CoSMoS system and validation of the wave and surge model within it using deep water wave buoy data and tidal gauge measurements as ground truth validation material. The evaluation is presented as monthly error measures between computed parameters and observed ones. Hindcast results over the whole year of 2009 show that the simulated wave parameters and surge elevation from the CoSMoS are in good agreement with data, with average root mean square error over the year of 0.14 m for the surge elevation and 0.24 m for the significant wave height. It is noted that there is a tendency of the wave model to underestimate the height of northerly waves with lower frequencies (swell). Additionally, when a wave separation algorithm is applied on the overall spectrum, results show consistent underestimation of the swell component by the model, which for the Dutch Coast, will mainly come from the North where the North Sea is open to the Atlantic Ocean. In the proposed model system, the swell boundary can have a significant effect on the simulated wave results, suggesting room for improvement for the swell boundary conditions on the North and the swell propagation within the Dutch Continental Shelf Model. Finally we show that in forecast mode, CoSMoS can provide reasonably good wave and surge prediction.

NHESSD

2, 3251–3288, 2014

1 Introduction

Knowledge of the actual condition of nearshore and coastal hydrodynamics is an essential point in coastal risk management and monitoring activities. Using this knowledge, the risk of coastal hazards, such as coastal inundation, beach and dune erosion, and rip currents can be predicted and mitigated. To this end, a coastal operational model system can serve as a key tool in providing recent and up-to-date information about the hydrodynamic and morphodynamic state of the coast. Output from such a model system can be valuable for coastal stake holders and decision makers. In this paper we apply CoSMoS (Coastal Storm Modeling System, Van Ormondt et al., 2012), an operational model system used here to predict storm impact on dunes along the Dutch Coast. The CoSMoS model system is generic and its application is not limited to storm impact prediction, but can be used to assess other coastal hazards, such as rip currents and flooding, in other environments. It was originally developed for simulating coastal inundation and erosion during winter storms along the Southern California coast (Barnard et al., 2009). Nowadays, many models are already available with which coastal processes and circulation can be simulated (Stelling, 1984; Van Dongeren et al., 1994; Wei et al., 1995; Roelvink et al., 2009). Model systems like CoSMoS can provide such coastal models with boundary information from larger area models in an efficient way and with low logistical efforts. In addition, meteorological data as input for CoSMoS can be obtained from well-established meteorological models, most of which are run in operational mode, e.g. GFS (Global Forecast System, operated by National Oceanic and Atmospheric Administration, USA), HIRLAM (High resolution limited area model, Unden et al., 2002), and ECMWF (European centre for medium-range weather forecast, Janssen et al., 1997).

Application of such model systems for wave forecasting has been demonstrated previously. On a global scale, Hanson et al., 2009 presented a skill assessment of three different regional wave models: WAM (Gunther, 2002), WAVEWATCH III (Tolman, 2009), and WAVAD (Resio and Perrie, 1989). They performed multi-decadal hindcasts for the

NHESSD
2, 3251–3288, 2014

Pacific Ocean, and found that in general, all three models show good skill, with WAVEWATCH III performing slightly better than the other two. For semi-enclosed basin scale modelling, some studies show that wave conditions can be well simulated in serious storm events (Mazarakis et al., 2012; Bertotti et al., 2011; Bertotti and Cavaleri, 2009; Cerneva et al., 2008). However, the quality of the wave model decreases substantially when the wind condition shows strong temporal and spatial gradients. This is particularly true for enclosed basins where an underestimation of wind speed by the atmospheric model is often found (Ponce de Leon and Soares, 2008; Cavaleri and Bertotti, 2004, 2006). In addition, wave models are very sensitive to small variations within the wind fields which act as forcing input (Bertotti and Cavaleri, 2009). Moreover, Cerneva et al. (2008) reported an underestimation by the WAM Cycle 4 model of significant wave heights in the case of low wind energy input and during combined swell-wind wave conditions. In contrast, the model shows relatively better performance for the case of high energy input. For the North Sea area, Behrens and Gunther (2009) demonstrated that WAM model that covers the North Sea and Baltic Sea, was capable to provide forecast 2 days ahead of winter storm Britta and Kyrill in 2006 with satisfactory results. As improvements to the model, they suggest further development on the atmospheric model (developed by German Weather Service). In addition to that, the model does not take into account depth induced wave breaking as one of the source terms in the model equation, which is a required further improvement necessary for a nearshore prediction system (Behrens and Gunther, 2009).

Application of such model systems as a coastal monitoring tool has also been demonstrated previously. Alvares-Elucaria (2010) developed an operational wave and current forecasting system for the north-eastern part of Mallorca Island mainly aimed at beach forecast conditions including rip currents. They make use of a 2DH Navier-Stokes model for the nearshore to generate surfzone waves and currents prediction. This model solves the mild slope equation, and derives its two dimensional wave spectra input from deep water wave prediction model WAM cycle 4, which is in turn forced by wind fields from HIRLAM. It is reported that during year of 2005–2007, the cor-

NHESSD
2, 3251–3288, 2014

relation between model prediction and measurements for the wave heights and mean period are 86 % and 78 %, respectively. A similar approach has also been implemented in Spain for monitoring application of beach nourishments (Gonzales et al., 2007).

The application of model systems for storm surge and tide prediction has also been demonstrated. For the Netherlands, Verlaan et al. (2005) make use of the hydrodynamic model, DCSM (Dutch Continental Shelf Model, Gerritsen et al., 1995) and forced it using meteorological model HIRLAM, to provide tide and storm surge forecasts. Moreover, they implemented an update to the Kalman filter configuration to improve quality of forecast, initially implemented by Heemink and Kloosterhuis (1990). This approach now has been applied in the operational prediction system Delft-FEWS (Delft-Flood Early Warning System, Werner et al., 2013), which has flexibility in integrating different models and data in a comprehensive way to provide forecast information. Specifically for coastal forecasting, De Kleermaeker et al. (2012) present an operational model system for the Dutch Coast under the framework of the FEWS system, combining data from different sources to provide a reliable forecast. They use the hydrodynamic model of Delft3D-FLOW to compute tides and surge and SWAN (Booij et al., 1999) for the waves. Preliminary results from the model system give a wave height bias of 10 % and root mean square error of 3.7 cm for the water levels.

For coastal monitoring purposes along the Dutch Coast, Baart et al. (2009) introduced a real time forecasting operational system in order to predict and hindcast morphological storm impacts. Using a similar forecast system, Van Ormondt et al. (2012) demonstrated the potential of such a system to forecast dune and beach erosion during storms, and hazardous swimming conditions during calmer weather. Particularly for swimmer safety applications, supplying CoSMoS with data from beach cameras to obtain up-to-date nearshore bathymetry also shows potential to be applied fully operationally (Van Dongeren et al., 2013).

In this paper, the CoSMoS application to the North Sea basin and validation will be presented. The system itself is similar to the one that is described in Baart et al. (2009) and Van Ormondt et al. (2012). The validation will be on the wave parameters

NHESSD
2, 3251–3288, 2014

and surge elevation simulated by the model, focussing on the Continental Shelf Model. The emphasis of the validation will be on the operational monthly performance. This paper is organized as follows: Sect. 2 describes the CoSMoS set up and description of models within it. Section 3 describes briefly methodologies and data that are used in the paper. In Sect. 4, results of the validation will be presented and discussed. Finally, conclusions will be drawn in Sect. 5.

2 CoSMoS set up and model description

The CoSMoS system is set up for the North Sea basin where regional wave and surge models are integrated with local (high resolution) models (Baart et al., 2009, van Ormondt et al., 2012). The model and domain structure of CoSMoS appears in Fig. 1. For the global model, Wave Watch III (WW3 from here on) is used, which solves the action density balance equation. WW3 is forced by GFS meteo data and generates 2-D wave spectra at particular locations as output. These outputs are used as boundary conditions for the nested models, as indicated in Fig. 1 by the arrows

The next nested model is the Dutch Continental Shelf Model (DCSM) which comprises the wave model SWAN and the surge model Delft3D-FLOW. The spatial resolution of the surge model is approximately 7.5 km × 10 km, while the resolution of the wave model is approximately 15 km × 20 km. The surge model is driven by meteo data from HIRLAM and amplitude and phase of several relevant tidal constituents are assigned using the tide model TPX072 (Egbert and Erofeeva, 2002). The SWAN model is forced by wind field from HIRLAM and the swell boundary conditions (area indicated by red lines in Fig. 2) are obtained from the global WW3 model. The models are run simultaneously, allowing for wave-current interactions. The model set up of the DCSM model within CoSMoS is summarized in Table 1, and model version and the parameter settings used in the model are presented in Table 2. For the wave model, whitecapping is modeled based on Westhuysen et al. (2007), bottom friction formula is from Hasselman et al. (1973), and depth induced wave breaking model is from Battjes and

NHESSD
2, 3251–3288, 2014

Janssen (1978). For the Delft3D FLOW model, uniform bed roughness coefficient is used, and wind drag coefficient is determined by a linear function of three break points and the corresponding wind speed (Delft3D FLOW User Manual). In this paper, The Dutch Coast Model and the Local Model will not be part of the analysis as we will focus on the application of CoSMoS for the North Sea.

The system is designed in a MATLAB platform, where the initiation and operational run are performed every 12 h, and managed by so called timer loop. There are two timer loops in the system that dictate the operational run. First, the main loop, which defines the starting time and end time of model run, triggers the overall initiation of the system, and downloads necessary wind and air pressure data to be used by the models. The second time loop is the model loop, in which model runs will be executed in sequence, starting from global and regional models followed by higher-resolution models. Downloaded forcing data and simulation results from the models are stored on a local OPeNDAP server (OPeNDAP: Open-source Project for a Network Data Access Protocol, Cornillon et al., 2003).

3 Data and method

The validation is carried out by comparing simulated parameters obtained from the model with the observed ones as ground truth. Statistical error measures are used to quantify the error between simulated and observed data. Here, root mean square error (e_{rms}), bias, and normalized error (e_{norm}) are used. The expressions are as follows:

$$e_{\mathrm{rms}} = \left[\frac{1}{N}\sum_{i=1}^{N}(x_i - y_i)^2\right]^{\frac{1}{2}} \quad (1)$$

$$\mathrm{bias} = \frac{1}{N}\sum_{i=1}^{N} x_i - \frac{1}{N}\sum_{i=1}^{N} y_i \quad (2)$$

NHESSD
2, 3251–3288, 2014

$$e_{\text{norm}} = \frac{\left[\frac{1}{N}\sum_{i=1}^{N}\left[(x_i - \overline{x}) - (y_i - \overline{y})\right]^2\right]^{\frac{1}{2}}}{\overline{y}} \quad (3)$$

In the Eqs. (1)–(3), N is the length of the time series parameter, x and y are simulated and observed parameter respectively, $\overline{x}$ and $\overline{y}$ are mean value of x and y respectively. For directional data, circular correlation and circular bias are used as statistical error measures. The circular bias is defined by subtracting the mean angular of the computed parameter from the mean angular of the observed. Here, the mean angular is computed by transforming the directional data into two vector components with magnitude of unity, and then taking the four quadrant inverse tangent of the resultant of the vectors as the mean angular (Berens, 2009). Circular correlation is computed by defining correlation coefficient of the directional data by also making use of the mean angular measures. Circular correlation (CC) and circular bias (CB) are defined as follows (Berens, 2009; Fisher, 1996):

$$\text{CC} = \frac{\sum_{i=1}^{N}\sin(x_i - \hat{x})\sin(y_i - \hat{y})}{\sqrt{\sum_{i=1}^{N}\sin^2(x_i - \hat{x})\sin^2(y_i - \hat{y})}} \quad (4)$$

$$\text{CB} = \hat{x} - \hat{y} \quad (5)$$

$$\hat{x} = \arctan(\boldsymbol{R}) \quad (6)$$

$$\boldsymbol{R} = \frac{1}{N}\sum_{i=1}^{N}\begin{bmatrix}\cos(m_i)\\ \sin(n_i)\end{bmatrix} \quad (7)$$

In the Eqs. (4)–(7), $\hat{x}$ and $\hat{y}$ are the mean angular of simulated and observed parameter respectively, (m, n) is the plane component of the directional data (unit vector), and $\boldsymbol{R}$ is the mean resultant vector.

NHESSD
2, 3251–3288, 2014

As the ground truth, data from deep water directional wave buoys and tidal gauge record are used, of stations located near the Dutch Coast. Three wave buoys are considered: Eierlandse Gat (EIELSGT), K13 Platform (K13APFM), and Euro Platform (EURPFM). For water levels, five gauges are used: Euro platform, Hoek van Holland, IJmuiden, Huibertgat, and K13 platform (Table 3 and Fig. 2). Data obtained from the buoys are processed, stored and retrievable as wave energy density, mean wave direction, and directional spreading as function of frequency, rather than the full 2-D spectra. Therefore, quasi 2-D wave energy spectrum is constructed using following expressions:

$$E(f,\theta) = E(f) \cdot D(\theta, f) \tag{8}$$

Where $E(f,\theta)$ is the wave energy as a function of frequency and direction and D is directional spreading. Since:

$$\int\int E(f,\theta)\mathrm{d}f\,\mathrm{d}\theta = \int E(f)\mathrm{d}f \tag{9}$$

therefore,

$$\int D(\theta,f)\mathrm{d}\theta = 1 \tag{10}$$

For the directional spreading, a normal distribution function is used:

$$D(\theta,f) = \frac{1}{\sigma\sqrt{2\pi}} \exp\left[\frac{\left[\theta - \theta_0(f)\right]^2}{2\sigma(f)^2}\right] \tag{11}$$

where $\theta_0(f)$ is mean direction as function of frequency, σ is directional spreading as function of frequency, and θ is the running wave direction. Here we have to keep in mind that the shape of the directional spreading function is assumed to be Gaussian

NHESSD
2, 3251–3288, 2014

and directional bimodality is not significant over the period of the data (Longuet-Higgins et al., 1963; Wenneker and Smale, 2013).

Since the wave model SWAN returns output as two-dimensional wave spectra as well, consistent parameter definitions can be used for both simulated and observed data. The integral wave parameters then will be calculated as follow:

$$H_{m0} = 4\sqrt{\int\int E(f,\theta)\mathrm{d}f\,\mathrm{d}\theta} \tag{12}$$

$$T_{\mathrm{p}} = \frac{1}{f_{\mathrm{p}}} \tag{13}$$

For the mean wave direction, formula from Kuik et al. (1988) is used:

$$\theta_{\mathrm{mean}} = \arctan\left[\frac{\int\int \sin\theta E(f,\theta)\mathrm{d}f\,\mathrm{d}\theta}{\int\int \cos\theta E(f,\theta)\mathrm{d}f\,\mathrm{d}\theta}\right] \tag{14}$$

For analysis purposes, in addition to bulk wave parameters, wind sea and swell components will also be computed. To this end, an algorithm will be applied on the total wave spectrum to differentiate between energy that belongs to wind sea and swell. The algorithm will largely follow Portilla et al. (2009) and Hanson et al. (2009). Here, for simplification we make an assumption that the total energy content in the spectrum only consists of one system of wind sea and one system of swell. The demarcation line between sea and swell is defined as:

$$f_{\mathrm{c}} = \frac{g}{2\pi}[\alpha U\cos(\delta)]^{-1} \tag{15}$$

$$0 \le \delta \le \frac{\pi}{2}$$

where f_{c} is the critical frequency, α is a constant, U is wind speed, and δ is the angle between wind sea and the wind. Energy content above this line will be counted as wind sea spectrum while below it is swell. The calibration parameter α of 1.8 is used.

NHESSD
2, 3251–3288, 2014

4 Results and discussion

4.1 Hindcast

A hindcast was performed for the calendar year of 2009, where the forcing for the model system is provided by the analyzed wind fields. In general, the year 2009 exhibited typical yearly wave conditions for the North Sea without any particular significant storm event. As we are interested in operational daily performance rather than specific event analysis, this particular year is thus a representative one. Weekly averaged observed significant wave height varied from 0.5 m during week 27 (month of July) up to 2.8 m during week 48 (month of November). For the latter period, the maximum observed wave height was 4.79 m. These wave heights are approximately in the same range for the three buoys considered.

4.1.1 Water level and surge validation

Model performance for water level and surge is analyzed by comparing both the simulated tidal signal and the surge with the observations. The surge levels were determined by subtracting astronomical prediction from the tidal signal. Results show that simulated tide and surge levels are in good agreement with observations. Figure 3 presents water levels plot for location IJmuiden during the storm that occurred in the last week of November 2009, where the computed water level (green) and observed water level (blue) elevates from astronomical prediction (grey). This water level raising is clearly seen from the observed surge level (black) which in a good agreement with the computed surge (red). Monthly error plots for the surge levels appear in Fig. 4. Root mean square error (left panel) vary from 0.09 m for station K13 platform for the month of September, until 0.21 m for station Europlatform for the month of March. For the bias (right panel), the highest positive value is found at station Huibertgat for the month of February with a bias of 0.12 m, while the strongest negative bias of −0.08 m is given by station K13 platform for the month of June. The relatively higher surge rms error coin-

NHESSD
2, 3251–3288, 2014

cides with the winter period where stormier and higher wind speeds are expected. This seasonal trend is clearly seen in Fig. 4, where all the tidal gauges considered show a similar tendency of lower rms error during summer months with relatively higher rms error during winter months. An exception is station K13 platform, where the rms error is relatively constant around 0.05 to 0.1 m over the year. This is due to the location of K13 platform which is relatively far offshore, which makes it less prone to the variability of wind driven surge. In addition, the results also show that stronger positive bias is found mainly during winter period, while during calmer months the absolute bias is relatively smaller with a tendency of being negative. Overall, the surge is in good agreement with observation over the year.

In addition, a tidal analysis was performed towards the computed water level where the amplitude and the phase of several relevant tidal constituents are compared with observations. Figure 5 presents a bar-plot of the tidal amplitude for six most dominant tidal constituents at the Dutch Coast. For the most important constituent, the M2, model (red) tends to slightly over predict the observations (black), except for stations K13 platform. Relative error is from 0.4 % for IJmuiden until 9 % for K13 platform. Similar to Fig. 5, in Fig. 6 the bar-plot of tidal phase is presented. Tidal phase is predicted well by the model, with higher error tendency appears in diurnal constituents K1 and O1. Absolute differences between computed phase and observations for the most important constituent M2 is 2 ° for K13 platform until 8 ° for IJmuiden.

4.1.2 Wave validation

In general, the wave model shows good skill in reproducing the wave parameters for the hindcast period. Examples of time series plots with simulated and observed wave parameters for K13 platform are presented in Fig. 7, where a storm occurred at the end of November. The wave height, peak period and mean wave direction computed by the wave model (blue) are in good agreement with the observations (red dots) over the two-week period that is shown, with a slight overestimation tendency of the observed wave height by the model. Monthly wave parameter errors are given in Fig. 8 for all

NHESSD
2, 3251–3288, 2014

the buoys considered. Over the whole year, the root mean square error (Fig. 8a, left panel) ranges from 0.16 m (Eierlandse Gat, month of May) until 0.35 m (Europlatform, month of November). The normalized error for the wave height (Fig. 8a, right panel) is consistently below 0.3 with bias in a range of −0.15 m to 0.15 m (Fig. 8a, middle panel). For the peak wave period (Fig. 8b), the rms error ranges from 1 s at the Europlatform buoy for the month of November, to 2.1 s at Eierlandse Gat for the month of September (Fig. 8b, left panel). The bias for the peak wave period is consistently negative (Fig. 8b, middle panel), ranging from −1.05 s up to −0.08 s for all buoys considered, suggesting that the model gives a consistent underestimation of peak wave period over the hindcast time. For the mean wave direction, model results show a significant agreement with the observations (Fig. 8c). The circular correlation varies from 0.7 at Europlatform and Eierlandse Gat during the month of January, up to 0.9 for the most of the months, showing a high correlation between the model result and the observation. Bias varies between –16° and 9° with most of the months give bias approximately ±10°.

In Fig. 9, scatter plots of observed and computed wave height are presented, with different color indicating different peak wave period, for station K13 platform during relatively calm period (the month of June, Fig. 9a) and stormy period (the month of November, Fig. 9b). Six panels scatter plot in (a) and (b) indicate 60° bin of observed incoming wave direction. The results show that the wave model tends to underestimate northerly waves with peak wave period greater than 7 s (blue and red scatter dots in Fig. 9a top-left panel, in Fig. 9b top-left and bottom-right panel). For semi enclosed seas like the North Sea, the wave climate will be dominated by wind waves while occasional swells can be expected to be present that mainly come from the North, where the shelf is open to the northern part of the Atlantic Ocean. From the results, it is shown that for waves with peak period greater than 7 s and coming from the North (between 330 and 30 nautical degree), there is a consistent tendency of the wave model to underestimate the wave height. In contrast, waves that come from West/South West do not suffer from this underestimation (direction between 150–210° and 210–270° in both Fig. 9a and b). This tendency is observed in all the buoys considered.

NHESSD
2, 3251–3288, 2014

When the wave separation algorithm is applied, the swell and wind sea component results show fairly good agreement with observations. In Fig. 10 monthly error and bias of swell height component (upper row) and wind sea height component (lower row) are presented. For the wind sea component, the bias is between −0.14 m and 0.19 m (middle panel lower row in Fig. 10), which is in contrast with the swell height bias that remains negative over the whole year (middle panel upper row in Fig. 10). This suggests again that the wave model underestimate swells, which may result in underestimation of northerly waves at the Dutch Coast.

4.1.3 Effect of swell boundary as model system component

The CoSMoS system applies the global WAVEWATCH III model to derive the swell boundary conditions for the DCSM model (red lines in Fig. 2). Here, a simulation is performed where we ignore the swell boundary and use only wind forcing from HIRLAM as the main input into the wave model to see the effect of such scenario. The result shows that model performance degrades after removal of the swell boundary with different reaction from the model for different periods. Figure 11 presents time series of wave height with and without the swell boundary for the month of June (left panel) and the month of November (right panel) for station Eierlandse Gat. During the month of June (Fig. 11, left panel), the degradation after ignoring the swell boundary is fairly significant, where the simulation result (red) suffers more underestimation compared to default setting of the model system (blue). The normalized root mean square error increases (on average over the buoys) by 34 %. In contrast, during the month of November (Fig. 11, right panel), the effect on negating the swell boundary is twice less than the month of June, with 15 % increase in normalized rms error.

4.2 Validation in forecast mode

In order to assess the capability of CoSMoS to predict events a number of days into the future, a forecast mode validation is performed where the model system is forced

NHESSD
2, 3251–3288, 2014

by HIRLAM forecast winds of the year 2009. Two types of forecast HIRLAM wind fields are considered: a 24 h forecast and a 48 h forecast. Figure 12 shows an example of surge elevation plots for different HIRLAM inputs together with the observations for IJmuiden during November 2009. Results using the HIRLAM forecasts both for 24 h and 48 h ahead (red and green line respectively) retain good agreement with observations (black dots). Differences are relatively small between results using analyzed wind (blue) and results using either the 24 or 48 h forecasted wind. Monthly error plots of surge elevation for different HIRLAM are shown in Fig. 13 for station IJmuiden. A strong seasonal feature is retained where a relatively lower rms error and bias exhibited during summer season while stronger bias is seen during summer period. The greatest rms error increase is 33 % (from analyzed to 48 h) for the month of December. On average, the rms error increases by 11 % (from analyzed to 24 h) and 25 % (from analyzed to 48 h) for all stations.

For the wave model, time series of wave heights for different HIRLAM forcings are presented in Fig. 14, for five days in the last week of November for location K13 platform, when the highest weekly-averaged wave heights were observed. The forecast results (red: 24 h, green: 48 h) are also in good agreement with observations (black dots). However, there are clear differences, especially with the 48 h HIRLAM forecasts, while results using analyzed and 24 h HIRLAM look relatively similar. Monthly errors of significant wave height for different HIRLAM are shown in Fig. 15 for location K13 platform. The rms error tends to increase as the forecast horizon increases. For instance at K13 platform for the month of November, the rms error was 0.31 m with analyzed wind, and further increased to 0.46 m and 0.56 m with 24 and 48 h winds, respectively. On average, stronger error increments are more prominent during the winter period. In contrast, the monthly-averaged bias does not increase strongly as the forecast horizon increases. On average, the rms error increases by 20 % and 40 % for 24 and 48 h forecast, respectively for all locations.

NHESSD
2, 3251–3288, 2014

5 Conclusions

A CoSMoS model system covering the North Sea is built which can hindcast and forecast wave conditions and water levels for the area along the Dutch Coast. The system is designed in a generic way to accommodate and integrate different regional and local models. A validation is performed of the Dutch Continental Shelf Model (DCSM), using wave buoys and tidal gauges available along the Dutch Coast. Hindcasts are performed where the model system is forced by atmospheric model HIRLAM analysis. Results show that the surge elevation produced by the model is in good agreement with observations with rms error ranging from 0.09 m to 0.21 m. On average, the model tends to slightly overestimate surge levels, especially during the winter months. For the wave model, simulated wave parameters agree well with observations with relative error of 14 % until 30 %. However, model tends to underestimate swell height. Using default settings of the model system (swell boundary is included), a consistent underestimation is found for northerly waves with relatively low frequency, which is also supported by the wave separation algorithm. This suggests room for improvement for the swell boundary conditions on the North of the model domain.

In order to test the CoSMoS system in forecast mode, it has been forced by HIRLAM 24 h and 48 h forecasts. The model system is capable of predicting high wave events and storm surge up to two days in advance. However, the performance does degrade as the forecast horizon increases. A smaller error increase is found for the surge elevation than for the wave heights. For surge elevation, on average, the rms error increases by 11 % (from analyzed to 24 h) and 25 % (from analyzed to 48 h) for all stations. On the other hand, for the wave model, the rms error increases on average by 20 % and 40 % for 24 and 48 h forecast, respectively.

To summarize, we conclude that CoSMoS Duth Continental Shelf Model is a fit-for-purpose regional model to provide boundary conditions for coastal models with which we can model and predict coastal inundation, beach and dune erosion, and rip currents, which are the topic of further research.

NHESSD
2, 3251–3288, 2014

In the future, merging CoSMoS with more integrated operational forecast system like FEWS is recommended in order to have more accurate prediction on storm surge level since introducing data assimilation into the system will increase forecast quality.

Acknowledgements. This research has been carried out in the framework of project: Real-Time Safety on Sandy Coasts funded by the Flood Control 2015 research program (project code 2010.05), and the Deltares' strategic research program "Event-driven Hydro- and Morphodynamics" (project code 1202362). The authors thank Ivo Wenneker and Alfons Smale for valuable discussions, also for providing buoy data and useful algorithms that are used in this work.

References

Alvarez-Ellacuria, A., Orfila, A., Olabarrieta, M., Medina, R., Vizoso, G., and Tintoré, J.: A nearshore wave and current operational forecasting system, J. Coastal Res., 503–509, doi:10.2112/08-1133.1, 2010.

Baart, F., van der Kaaij, T., van Ormondt, M., van Dongeren, A., van Koningsveld, M., and Roelvink, J. A.: Real-time forecasting of morphological storm impacts: a case study in The Netherlands, J. Coastal Res., 56, 1617–1621, 2009.

Barnard, P., O'Reilly, B., van Ormondt, M., Elias, E., Ruggiero, P., Erikson, L., Hapke, C., Collins, B. D., Guza, R. T., Adams, P. N., and Thomas, J. T.: The framework of a coastal hazards model; a tool for predicting the impact of severe storms, US Geological Survey Open-File Report 2009–1073, 21 pp., 2009.

Battjes, J. A. and Janssen, J. P. F. M.: Energy loss and set-up due to breaking of random waves, 16th Int. Conf. Coast. Eng., ASCE, 569–587, 1978.

Behrens, A. and Günther, H.: Operational wave prediction of extreme storms in Northern Europe, Nat. Hazards, 49, 387–399, 2009.

Berens, P.: CircStat: a MATLAB toolbox for circular statistics, J. Stat. Softw., 31, 1–21, 2009.

Bertotti, L. and Cavaleri, L.: Wind and wave predictions in the Adriatic Sea, J. Marine Syst., 78, S227–S234, 2009.

Bertotti, L., Canestrelli, P., Cavaleri, L., Pastore, F., and Zampato, L.: The Henetus wave forecast system in the Adriatic Sea, Nat. Hazards Earth Syst. Sci., 11, 2965–2979, doi:10.5194/nhess-11-2965-2011, 2011.

NHESSD

2, 3251–3288, 2014

Booij, N., Ris, R. C., and Holthuijsen, L. H.: A third-generation wave model for coastal regions 1. Model description and validation, J. Geophys. Res., 104, 7649–7666, 1999.
Cavaleri, L. and Bertotti, L.: Accuracy of the modelled wind and wave fields in enclosed seas, Tellus A, 56, 167–175, 2004.
Cavaleri, L. and Bertotti, L.: The improvement of modelled wind and wave fields with increasing resolution, Ocean Eng., 33, 553–565, 2006.
Cherneva, Z., Andreeva, N., Pilar, P., Valchev, N., Petrova, P., and Guedes Soares, C.: Validation of the WAMC4 wave model for the Black Sea, Coast. Eng., 55, 881–893, 2008.
Cornillon, P., Gallagher, J., and Sgouros, T.: OPeNDAP: accessing data in a distributed, heterogeneous environment, Data Science Journal, 2, 164–174, 2003.
De Kleermaeker, S., Verlaan, M., Kroos, J., and Zijl, F.: A new coastal flood forecasting system for the Netherlands, Hydro12 – Taking care of the sea, 13–15 November 2012, Rotterdam, 2012.
Deltares: Simulation of multi-dimensional hydrodynamic flows and transport phenomena, including sediments, DELFT3D-FLOW User Manual, 2013.
Egbert, G. D. and Erofeeva, S. Y.: Efficient inverse modeling of barotropic ocean tides, J. Atmos. Ocean Tech., 19, 183–204, 2002.
Fisher, N. I.: Statistical Analysis of Circular Data, Cambridge University Press, 1996.
Gerritsen, H., de Vries, J. W., and Philippart, M. E.: The Dutch continental shelf model, in: In Quantitative Skill Assesment for Coastal Ocean, edited by: Lynch, D., and Davies, A., American Geophysical Union, Washington DC, 425–467, 1995.
González, M., Medina, R., Gonzalez-Ondina, J., Osorio, A., Méndez, F. J., and García, E.: An integrated coastal modeling system for analyzing beach processes and beach restoration projects, SMC, Comput. Geosci., 33, 916–931, 2007.
Gunther, H.: WAM Cycle 4.5., Institute for Coastal Research, GKSS Research Centre, Germany, 2002.
Hanson, J. L., Tracy, B. A., Tolman, H. L., and Scott, R. D.: Pacific hindcast performance of three numerical wave models, J. Atmos. Ocean Tech., 26, 1614–1633, 2009.
Hasselman, K., Barnett, T. P., Bouws, E., Carlson, D. E., and Hasselmann, P.: Measurements of wind-wave growth and swell decay during the Joint North Sea Wave Project (JONSWAP), Deutsche Hydrographische Zeitschrift, 8, 1973.
Heemink, A. W. and Kloosterhuis, H.: Data assimilation for non-linear tidal models, Int. J. Numer. Meth. Fl., 11, 1097–1112, 1990.

NHESSD
2, 3251–3288, 2014

Janssen, P. A. E. M., Hansen, B., and Bidlot, J.-R.: Verification of the ECMWF wave forecasting system against Buoy and altimeter data, Weather Forecast., 12, 763–784, 1997.
Kuik, A. J., van Vledder, G. P., and Holthuijsen, L. H.: A method for the routine analysis of pitch-and-roll Buoy wave data, J. Phys. Oceanogr., 18, 1020–1034, 1988.
Longuet-Higgins, M. S. and Stewart, R. W.: A note on wave set-up, J. Mar. Res., 21, 4–10, 1963.
Mazarakis, N., Kotroni, V., Lagouvardos, K., and Bertotti, L.: High-resolution wave model validation over the Greek maritime areas, Nat. Hazards Earth Syst. Sci., 12, 3433–3440, doi:10.5194/nhess-12-3433-2012, 2012.
Ponce de León, S. and Guedes Soares, C.: Sensitivity of wave model predictions to wind fields in the western Mediterranean Sea, Coast. Eng., 55, 920–929, 2008.
Portilla, J., Ocampo-Torres, F. J., and Monbaliu, J.: Spectral partitioning and identification of wind sea and swell, J. Atmos. Ocean Tech., 26, 107–122, 2009.
Resio, D. and Perrie, W.: Implications of an f-4 equilibrium range for wind-generated waves, J. Phys. Oceanogr., 19, 193–204, 1989.
Roelvink, D., Reniers, A., van Dongeren, A., van Thiel de Vries, J., McCall, R., and Lescinski, J.: Modelling storm impacts on beaches, dunes and barrier islands, Coast. Eng., 56, 1133–1152, 2009.
Stelling, G.: On the construction of computational methods for shallow water flow problems, Rijkswaterstaat communication no.35, The Hague, 1984.
Tolman, H. L.: User manual and system documentation of WAVEWATCH-III version 3.14., 2009.
Unden, P., Rontu, L., Jarvinen, H., Lynch, P., Calvo, J., Cats, G., Cuxart, J., Eerola, K., Fortelius, C., Garcia-Moya, J. A., Jones, C., Lenderlink, G., McDonald, A., McGrath, R., Navascues, B., Nielsen, N. W., Degaard, V., Rodriguez, E., Rummukainen, M., Sattler, K., Sass, B. H., Savijarvi, H., Schreur, B. W., Sigg, R., and The, H.: HIRLAM-5 Scientific Documentation, 2002.
Van Dongeren, A., Sancho, F. E., Svendsen, I. A., and Putrevu, U.: SHORECIRC: a quasi 3-D nearshore model, Coast. Eng., 2741–2754, 1994.
Van Dongeren, A., Van Ormondt, M., Sembiring, L., Sasso, R., Austin, M., Briere, C., Swinkels, C., Roelvink, D., and Van Thiel de Vries, J.: Rip current predictions through model data assimilation on two distinct beaches, Coastal Dynamics, Bordeaux University, Bordeaux, France, 2013.

NHESSD
2, 3251–3288, 2014

Van Ormondt, M., Van Dongeren, A., Briere, C., Sembiring, L., Winter, G., Lescinski, J., and Swinkels, C.: Simulating storm impacts and coastal flooding along the Netherlands coast, in: Flood Risk 2012, Rotterdam, the Netherlands, 28–29, 2012.

Verlaan, M., Zijderveld, A., de Vries, H., and Kroos, J.: Operational storm surge forecasting in the Netherlands: developments in the last decade, Philos. T. R. Soc. A, 363, 1441–1453, 2005.

Wei, G., Kirby, J. T., Grilli, S. T., and Subramanya, R.: A fully nonlinear Boussinesq model for surface waves. Part 1. Highly nonlinear unsteady waves, J. Fluid Mech., 294, 71–92, 1995.

Wenneker, I. and Smale, A.: Measurement of 2D wave spectra during a storm in a tidal inlet, Coastal Dynamics, France, 2013.

Werner, M., Schellekens, J., Gijsbers, P., van Dijk, M., van den Akker, O., and Heynert, K.: The Delft-FEWS flow forecasting system, Environ. Modell. Softw., 40, 65–77, 2013.

Westhuysen, A. J., Zijlema, M., and Battjes, J. A.: Nonlinear saturation-based whitecapping dissipation in SWAN for deep and shallow water, Coast. Eng., 54, 151–170, 2007.

NHESSD

2, 3251–3288, 2014

Table 1. Model set up for DCSM.

	SWAN	Delft3D Flow
Grid size	~ 15 km × 20 km	~ 7.5 km × 10 km^2
Open boundary	WAVEWATCH III Global	Tide model TPX072
Meteo input	HIRLAM	HIRLAM
Source term:		–
Wind growth	Westhuysen et al. (2007)	
White capping	Westhuysen et al. (2007)	
Bottom friction	JONSWAP (Hasselman et al., 1973)	
Depth induced breaking	Battjes and Janssen (1978)	

NHESSD
2, 3251–3288, 2014

Table 2. Model version and parameter settings.

SWAN, model version 4072 Source term	Value
Whitecapping (Westhuysen et al., 2007)	
B_R (threshold saturation level)	0.00175
C'_{ds} (proportionality coefficient)	0.00005
Bottom friction (Hasselman et al., 1973)	
C (bottom friction coefficient)	$0.067\,m^2\,s^{-3}$
Depth induced breaking (Battjes and Janssen, 1978)	
Gamma (breaker parameter)	0.73
Alpha (dissipation coefficient)	1.0
DELFT 3-D FLOW, model version 4.01	
Bed roughness Chezy coefficient	$90\,m^{1/2}\,s^{-1}$
Wind drag coefficient A, B, C (see Delft3D User Manual)	0.00063, 0.00723, 0.00723

NHESSD
2, 3251–3288, 2014

Table 3. Stations used in validation.

Station	Name	Abbreviation in this paper	Type
B1	Eierlandse Gat	EIELSGT	Directional wave buoy
B2	Euro platform	EURPFM	Directional wave buoy
B3	K13 platform	K13APFM	Directional wave buoy
T1	Euro platform	EUR	Tidal gauge
T2	Hoek van Holland	HvH	Tidal gauge
T3	IJmuiden	IJM	Tidal gauge
T4	Huibergat	HUI	Tidal gauge
T5	K13 platform	K13	Tidal gauge

NHESSD
2, 3251–3288, 2014

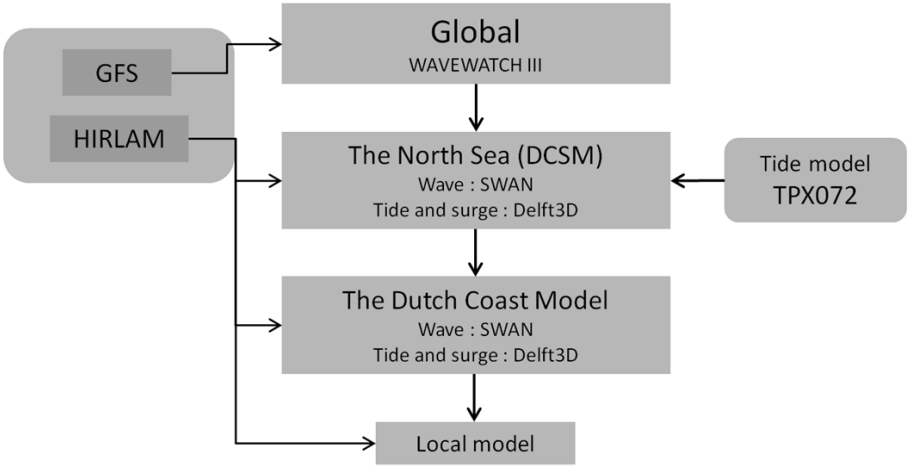

Fig. 1. Model and domain structure within CoSMoS.

NHESSD
2, 3251–3288, 2014

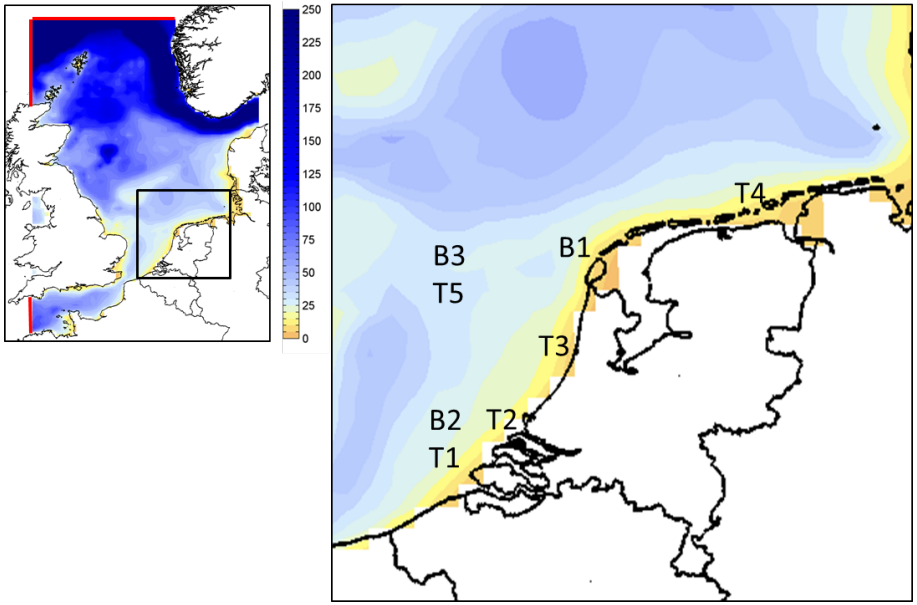

Fig. 2. The North Sea (left), with the colour shading represents depth. Red lines indicate the swell boundary for the wave model. The Dutch Coast (right), and stations used in analysis (see Table 3).

NHESSD
2, 3251–3288, 2014

A validation of an operational wave and surge prediction system

L. Sembiring et al.

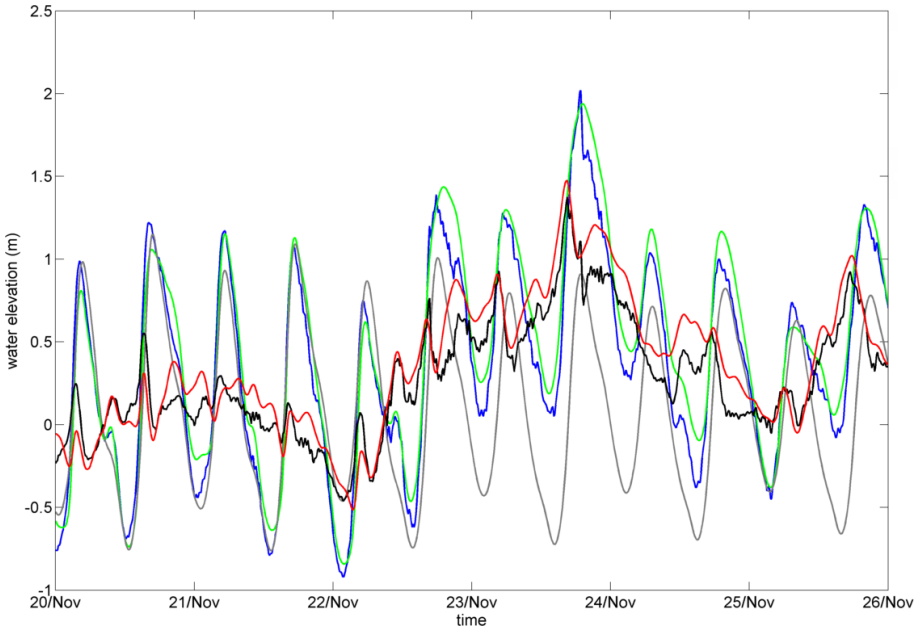

Fig. 3. Water elevation for IJmuiden during the storm in November 2009, blue: observed water level, green: computed water level, black: observed surge, red: computed surge, grey: astronomical prediction.

NHESSD
2, 3251–3288, 2014

A validation of an operational wave and surge prediction system

L. Sembiring et al.

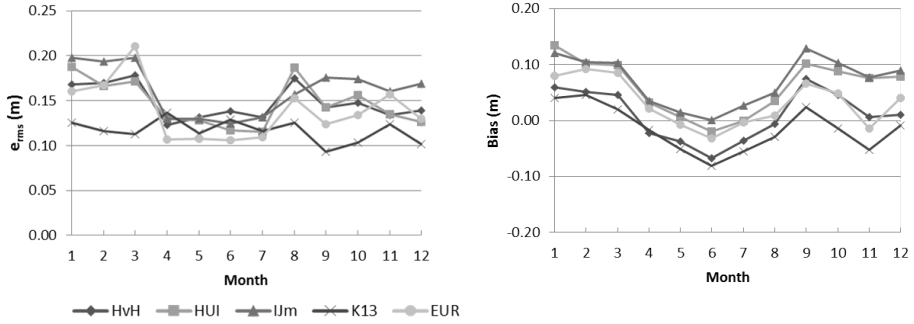

Fig. 4. Monthly root mean square error (left) and bias (right) of surge elevation.

NHESSD
2, 3251–3288, 2014

A validation of an operational wave and surge prediction system

L. Sembiring et al.

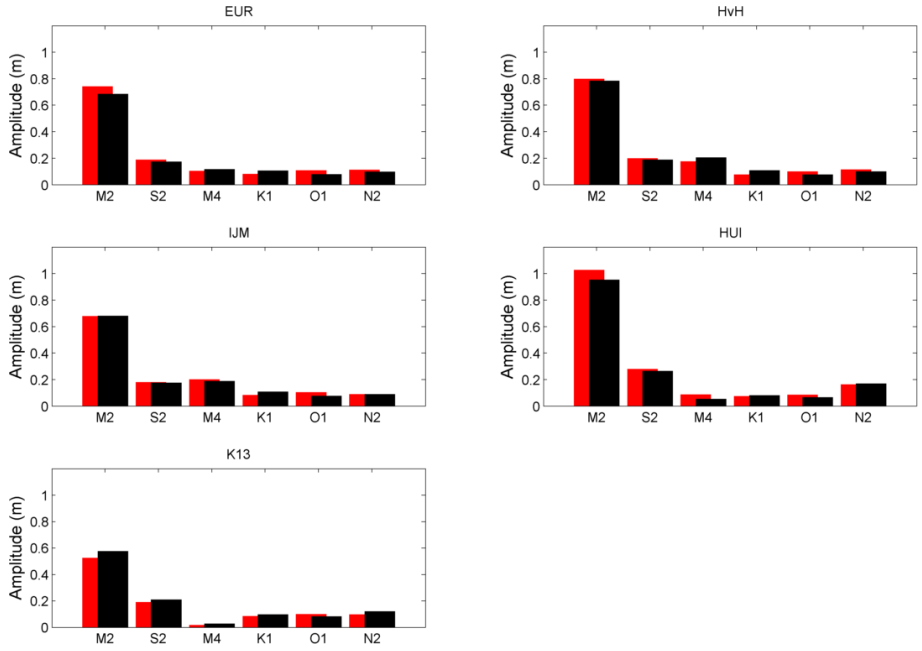

Fig. 5. Tidal amplitude comparison for six tidal constituents, black: observation, red: computed.

NHESSD
2, 3251–3288, 2014

A validation of an operational wave and surge prediction system

L. Sembiring et al.

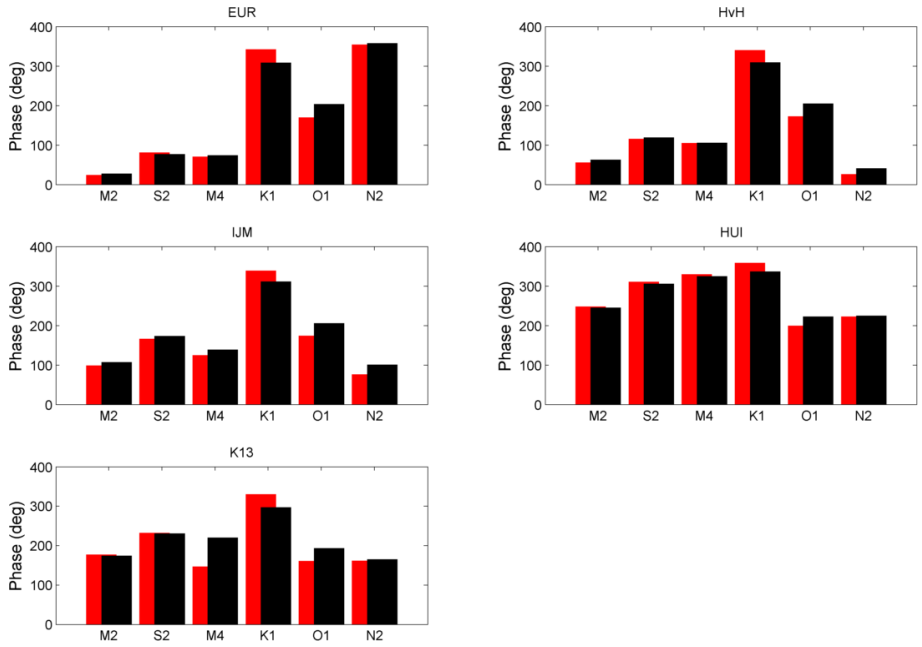

Fig. 6. Tidal phase comparison for six tidal constituents, black: observation, red: computed.

NHESSD
2, 3251–3288, 2014

A validation of an operational wave and surge prediction system

L. Sembiring et al.

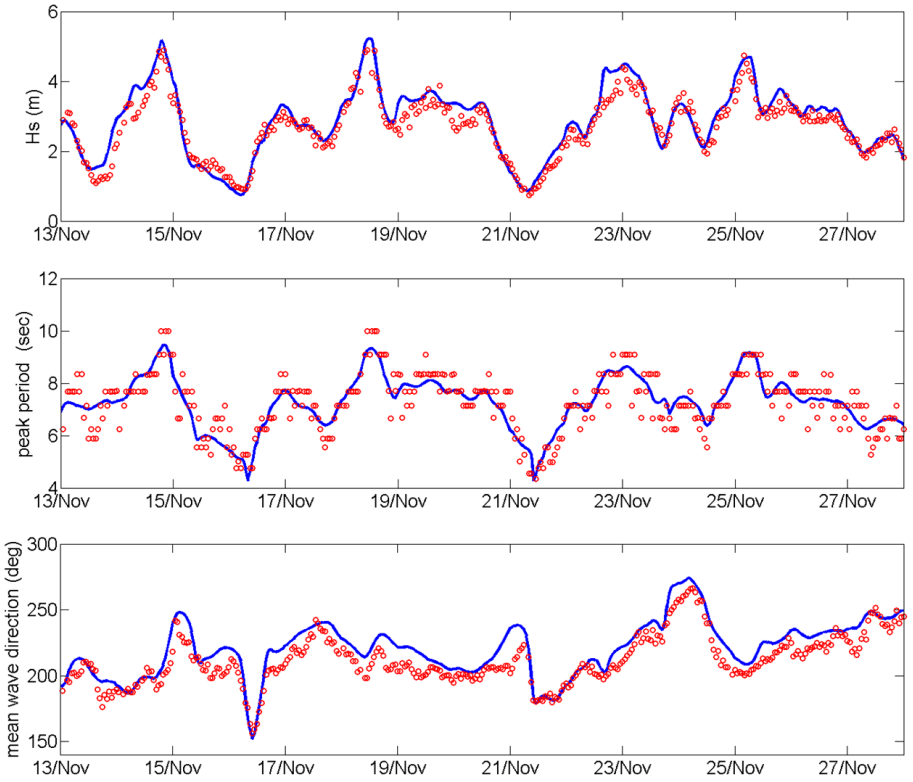

Fig. 7. Time series of wave parameters, blue: model results, red dots: observations. Wave height (upper panel), peak period (middle), and mean wave direction (lower). Location: K13 platform.

NHESSD
2, 3251–3288, 2014

A validation of an operational wave and surge prediction system

L. Sembiring et al.

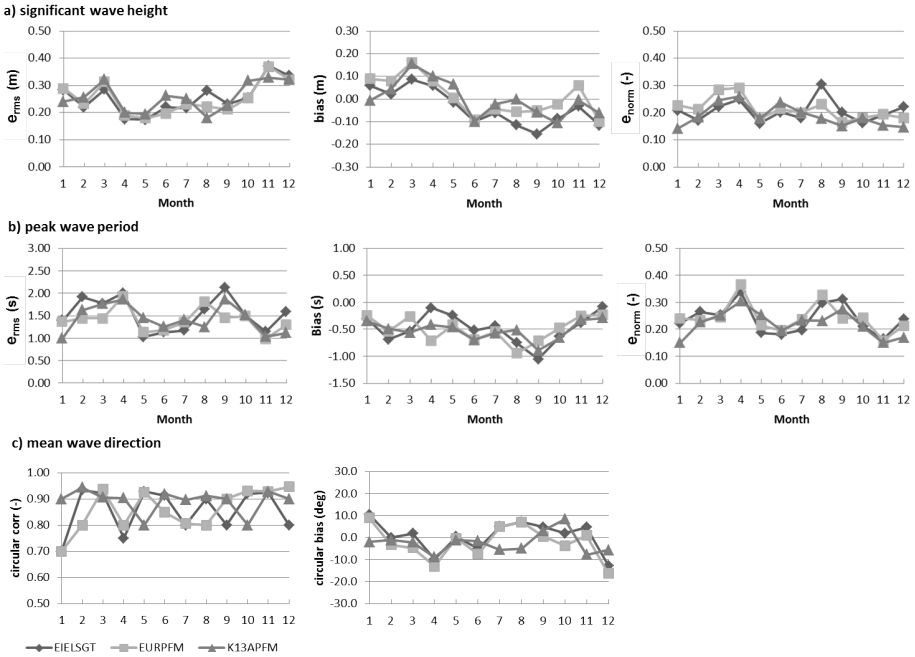

Fig. 8. Monthly errors of wave parameters, **(a)**: wave height, **(b)**: peak period, **(c)**: mean wave direction.

NHESSD
2, 3251–3288, 2014

A validation of an operational wave and surge prediction system

L. Sembiring et al.

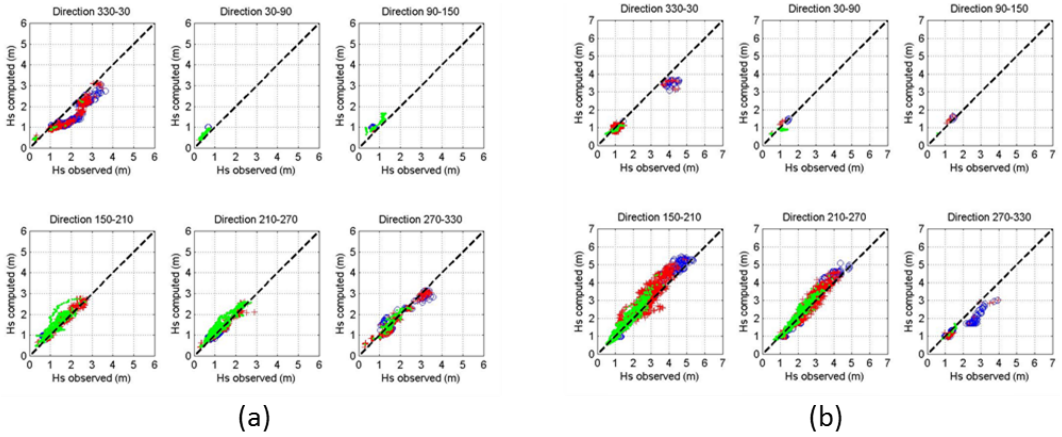

Fig. 9. Scatter plot of observed significant wave height H_s vs. computed, for every 60° of observed incoming mean wave direction, for different peak wave period, T_p. Green: observed H_s with $T_p < 7$ s, red: $7 < T_p < 9$ s, blue: $T_p > 9$ s. **(a)** month of July, **(b)** month of November. Location: K13 platform

NHESSD
2, 3251–3288, 2014

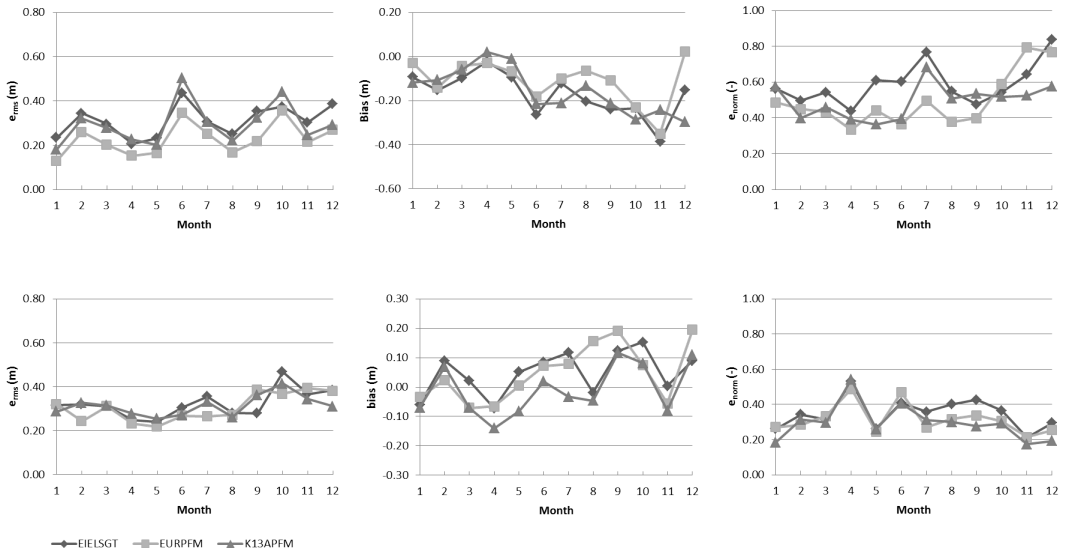

Fig. 10. Monthly errors of swell height (first row) and wind sea component (second row).

NHESSD
2, 3251–3288, 2014

A validation of an operational wave and surge prediction system

L. Sembiring et al.

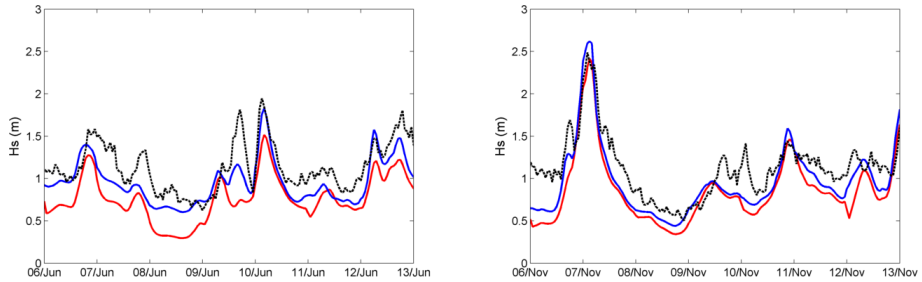

Fig. 11. Significant wave height H_s for Eierlandse Gat for the month of June (left) and November (right), black: observed; blue: with swell boundary; red: without swell boundary.

NHESSD
2, 3251–3288, 2014

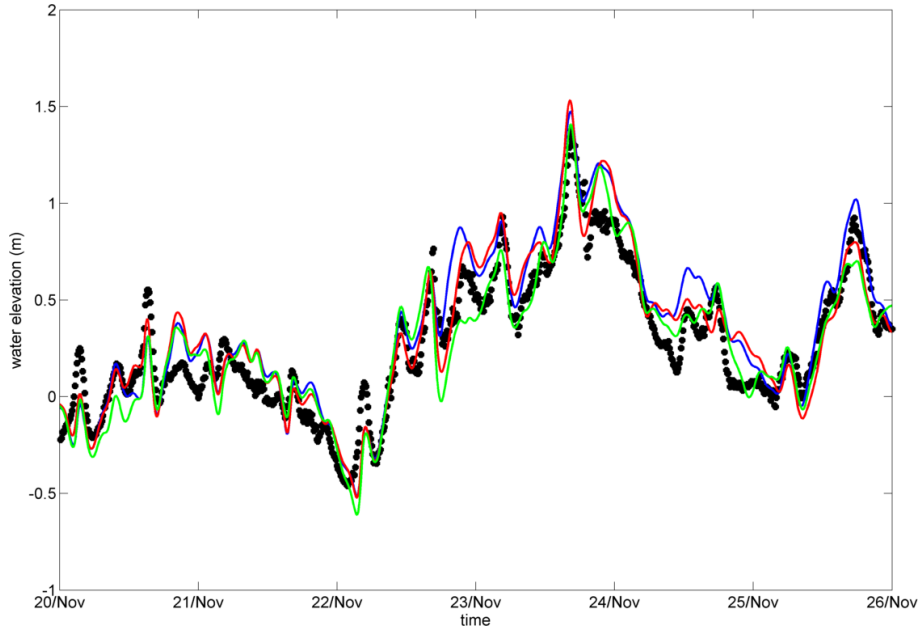

Fig. 12. Surge elevation for IJmuiden during the November 2009 storm using, blue: analysed HIRLAM; red: 24 h HIRLAM; green: 48 h HIRLAM; black dots: observation.

NHESSD
2, 3251–3288, 2014

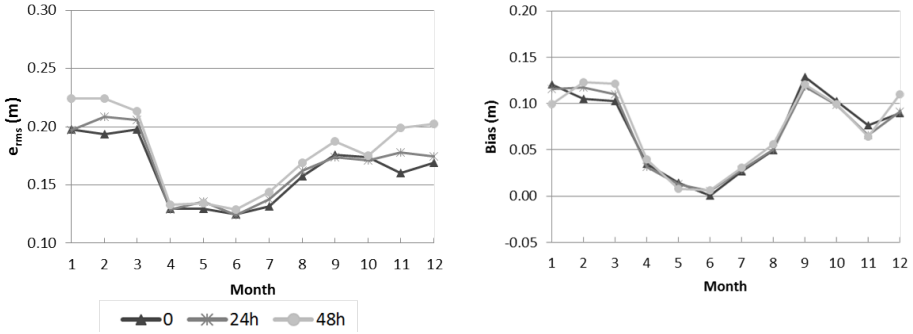

Fig. 13. Monthly errors of surge elevation for different HIRLAM for location IJmuiden.

NHESSD
2, 3251–3288, 2014

A validation of an operational wave and surge prediction system

L. Sembiring et al.

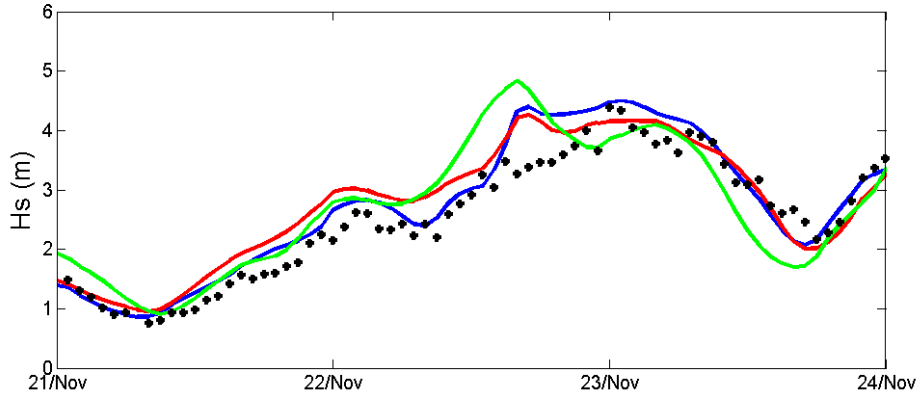

Fig. 14. Significant wave height H_s for different HIRLAM input, blue: analyzed; red: 24 h forecast; green: 48 h forecast; black dots: buoy. Location: K13 platform.

NHESSD
2, 3251–3288, 2014

A validation of an operational wave and surge prediction system

L. Sembiring et al.

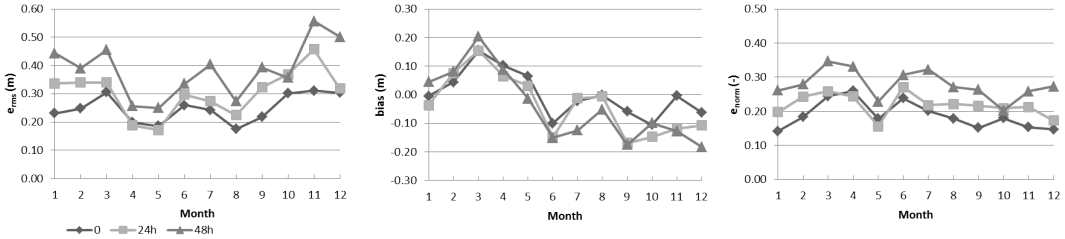

Fig. 15. Monthly error of significant wave height H_s for different HIRLAM input, location K13 platform.

NHESSD
2, 3251–3288, 2014

A validation of an operational wave and surge prediction system

L. Sembiring et al.